Supporting Information for:

A Theoretical Chemical Bonding, Vibronic Coupling and Magnetic Anisotropy in Linear Iron(II) Complexes With Single Molecule Magnet Behavior

Mihail Atanasov[1,2]*, Joseph M. Zadrozny[3], Jeffrey R. Long[3*] , Frank Neese[1]*

[1] Max-Planck Institut für Chemische Energiekonversion, Stiftstr. 32-34, D-45470 Mülheim an der Ruhr, Germany,
[2] Institute of General and Inorganic Chemistry, Bulgarian Academy of Sciences, Acad.Georgi Bontchev Str.11, 1113 Sofia, Bulgaria,

[3]Department of Chemistry, University of California, Berkeley, California, 94720, U. S. A.

Chem. Sci.

Table of Contents

SI.1 The Hamiltonian $\hat{H}_{BO}+\hat{H}_{SOC}+\hat{H}_{Z}$ in the basis of the $|M_L=\pm2, M_S=\pm2,\pm1,0\rangle$ basis functions, derivation of eigenvalues and g-tensor expressions.

The matrix of the Born-Oppenheimer Hamiltonian plus spin-orbit coupling plus the Zeeman operator $\hat{H}_{BO}+\hat{H}_{SOC}+\hat{H}_{Z}$ within the basis of products of orbital (M_L) and spin (M_S) functions $|M_L=\pm2, M_S=\pm2,\pm1,0\rangle$ for the ^5E ground states is:

$\|+2,+2\rangle$	$\|-2,+2\rangle$	$\|-2,-2\rangle$	$\|+2,-2\rangle$	$\|+2,+1\rangle$	$\|-2,+1\rangle$	$\|-2,-1\rangle$	$\|+2,-1\rangle$	$\|+2,0\rangle$	$\|-2,0\rangle$
$-\zeta+6\beta H_z$	$-\delta_1-i\delta_2$	0	0	$2\beta(H_x-iH_y)$	0	0	0	0	0
$-\delta_1+i\delta_2$	$\zeta+2\beta H_z$	0	0	0	$2\beta(H_x-iH_y)$	0	0	0	0
0	0	$-\zeta-6\beta H_z$	$-\delta_1+i\delta_2$	0	0	$2\beta(H_x+iH_y)$	0	0	0
0	0	$-\delta_1-i\delta_2$	$-\zeta-2\beta H_z$	0	0	0	$2\beta(H_x+iH_y)$	0	0
$2\beta(H_x+iH_y)$	0	0	0	$-\frac{\zeta}{2}+4\beta H_z$	$-\delta_1-i\delta_2$	0	0	$\sqrt{\frac{3}{2}}\beta(H_x-iH_y)$	0
0	$2\beta(H_x+iH_y)$	0	0	$-\delta_1+i\delta_2$	$\frac{\zeta}{2}$	0	0	0	$\sqrt{\frac{3}{2}}\beta(H_x-iH_y)$
0	0	$2\beta(H_x-iH_y)$	0	0	0	$-\frac{\zeta}{2}-4\beta H_z$	$-\delta_1+i\delta_2$	0	$\sqrt{\frac{3}{2}}\beta(H_x+iH_y)$
0	0	0	$2\beta(H_x-iH_y)$	0	0	$-\delta_1-i\delta_2$	$\frac{\zeta}{2}$	$\sqrt{\frac{3}{2}}\beta(H_x+iH_y)$	0
0	0	0	0	$\sqrt{\frac{3}{2}}\beta(H_x+iH_y)$	0	0	$\sqrt{\frac{3}{2}}\beta(H_x-iH_y)$	$2\beta H_z$	$-\delta_1-i\delta_2$
0	0	0	0	0	$\sqrt{\frac{3}{2}}\beta(H_x+iH_y)$	$\sqrt{\frac{3}{2}}\beta(H_x-iH_y)$	0	$-\delta_1+i\delta_2$	$-2\beta H_z$

(S1.1)

Without a magnetic field this matrix decomposes into five 2x2 matrices. For example focusing on the states $|2,2\rangle$ and $|-2,2\rangle$ we have :

$$\begin{bmatrix} -\zeta & -\delta_1 - i\delta_2 \\ -\delta_1 + i\delta_2 & \zeta \end{bmatrix}$$

Diagonalization yields:

$$E_{\pm} = \pm\sqrt{\zeta^2 + \delta^2}$$

In a similar way eigenvalues for the other pairs of states are obtained. They are listed in Table S1. Taking the component $|\pm 2,\pm 2\rangle$ of the ground state magnetic pair we get the following matrices of relevance for the calculation of the g-tensor components g_z and g_x, respectively(g_y=g_x);

g_z:

$$\begin{matrix} |2,2\rangle & |-2,2\rangle \\ \end{matrix}$$
$$\begin{bmatrix} -\zeta + 6\beta H_z & -\delta_1 - i\delta_2 \\ -\delta_1 + i\delta_2 & \zeta + 2\beta H_z \end{bmatrix} = 4\beta H_z \begin{bmatrix} 1 & 0 \\ 0 & 1 \end{bmatrix} + \begin{matrix} |2,2\rangle & |-2,2\rangle \\ \end{matrix} \begin{bmatrix} -\zeta + 2\beta H_z & -\delta_1 - i\delta_2 \\ -\delta_1 + i\delta_2 & -\zeta - 2\beta H_z \end{bmatrix} \quad \text{(S1.2)}$$

g_y=g_x:

$$\begin{matrix} |2,2\rangle & |2,1\rangle \\ \end{matrix}$$
$$\begin{bmatrix} -\zeta & 2\beta H_x \\ 2\beta H_x & -\frac{\zeta}{2} \end{bmatrix} = -(3/4)\zeta \begin{bmatrix} 1 & 0 \\ 0 & 1 \end{bmatrix} + \begin{matrix} |2,2\rangle & |2,1\rangle \\ \end{matrix} \begin{bmatrix} -\frac{\zeta}{4} & 2\beta H_x \\ 2\beta H_x & \frac{\zeta}{4} \end{bmatrix} \quad \text{(S1.3)}$$

Matrices S1.2 and S1.3 are represented in the form of a sum of a diagonal term and a baricentered term and lead to the following expressions for the dependence of the ground state eigenvalue on the H_z and H_x magnetic field directions:

$$E(H_z) = 4\beta H_z - \sqrt{(\zeta - 2\beta H_z)^2 + \delta^2} \quad \text{(S1.4)}$$

$$E(H_x) = -(3/4)\zeta - \sqrt{\frac{\zeta^2}{16} + 4\beta^2 H_x^2} \quad \text{(S1.5)}$$

where $\delta^2 = \delta_1^2 + \delta_2^2$ (see definitions for δ_1 and δ_2 in Section II.2). Following the definitions of g_z and g_x as the first der derivatives of the energy with respect to the respective components of the magnetic field:

$$g_z = \frac{2}{\beta}(\partial E / H_z)_{H_z=0} \quad \text{(S1.6)}$$

$$g_x = \frac{2}{\beta}(\partial E / H_x)_{H_x=0} \qquad \text{(S1.7)}$$

appropriate to a *s*=1/2 pseudospin-definition for the *g*-tensor. Using eqs. S1.6 and S1.7 and differentiating we obtain:

$$g_z = 8 + \frac{4\zeta}{\sqrt{\zeta^2 + \delta^2}} \qquad \text{(S1.8)}$$

$$g_x = 0 \qquad \text{(S1.9)}$$

Following the same recipe expressions for the *g*-tensors of the other states are obtained and listed in Table S1.

Table S1. Expressions for the Energies and the Anisotropic g_z-tensor Component of the Magnetic Sublevels split out from ^{5}E Ground State Energies by Spin-Orbit Coupling[a] and Off-Axial Ligand Field.[b]

$\lvert M_L, M_S \rangle$	$M_J = M_L + M_S$	Energy	g_z [c]
E, $\lvert \pm 2, \pm 2 \rangle$	±4	$-\sqrt{\zeta^2 + \delta^2}$	$\frac{4\zeta}{\sqrt{\zeta^2 + \delta^2}} + 8$
A_1,A_2 $\lvert \pm 2, \pm 1 \rangle$	±3	$-\sqrt{\frac{\zeta^2}{4} + \delta^2}$	$\frac{2\zeta}{\sqrt{\frac{\zeta^2}{4} + \delta^2}} + 4$
E $\lvert \pm 2, 0 \rangle$	±2	$\pm\delta$	0
E $\lvert \pm 2, \mp 1 \rangle$	±1	$\sqrt{\frac{\zeta^2}{4} + \delta^2}$	$-\frac{2\zeta}{\sqrt{\frac{\zeta^2}{4} + \delta^2}} + 4$
A_1,A_2 $\lvert \pm 2, \mp 2 \rangle$	0	$\sqrt{\zeta^2 + \delta^2}$	$-\frac{4\zeta}{\sqrt{\zeta^2 + \delta^2}} + 8$

[a] quantified by the spin-orbit coupling constant ζ; [b] quantified by the parameter $\delta = \sqrt{\delta_1^2 + \delta_2^2}$, see eqs.3-4 for definitions of δ_1 and δ_2; [c] g-tensor values are defined for pseudo spins $\pm 1/2$; non-listed values for $g_{x,y}$ are close to zero (δ<<ζ) or 8(δ>>ζ).

SI.2 Renner-Teller effect and solution of the vibronic energy eigenvalue problem.

The expression for the ground state potential energy for the ${}^5E\otimes\varepsilon$ RT effect is formally equivalent to quadratic ${}^5E\otimes\varepsilon$ Jahn-Teller coupling: [63-69]

$$\begin{matrix} \left|{}^5E(d_{x2-y2})\right\rangle & \left|{}^5E(d_{xy})\right\rangle & \left|{}^5E(d_{x2-y2})\right\rangle & \left|{}^5E(d_{xy})\right\rangle \end{matrix}$$

$$\hat{H}_{RT}+\hat{H}_{vib}=\begin{bmatrix} \frac{1}{2}g(Q_x^2-Q_y^2) & gQ_xQ_y \\ gQ_xQ_y & -\frac{1}{2}g(Q_x^2-Q_y^2) \end{bmatrix}+\begin{bmatrix} \frac{1}{2}K_\varepsilon(Q_x^2+Q_y^2) & 0 \\ 0 & \frac{1}{2}K_\varepsilon(Q_x^2+Q_y^2) \end{bmatrix} \qquad \text{(S2.1)}$$

with g and K_ε –representing the quadratic RT and force constants, respectively, and Q_x and Q_y –the components of the ε-normal mode. This splits the ${}^5E(\mathrm{d_{x2\text{-}y2,xy}})^1$ ground state surface into two sheets that are described by the simple expression:

$$E_\pm=\frac{1}{2}(K_\varepsilon\pm g)(Q_x^2+Q_y^2) \qquad \text{(S2.2))}$$

Depending on whether $K_\varepsilon > g$ or $K_\varepsilon < g$, two different situations are encountered (Figure 2). In the first case, no new minima in the adiabatic ground state potential energy surface (APES) arise; however, the adiabatic approximation is violated by the vibronic mixing (via the term gQ_xQ_y) between the two sublevels. The other extreme, $K_\varepsilon < g$, leads to a negative curvature for the lower surface, and therefore to dynamical instability. As a consequence, new minima on the APES corresponding to bent structures arise. To determine the distorted geometries and energy stabilizations at these new minima, higher-order vibronic terms need to be introduced. Traditionally this is most easily accomplished by introducing one diagonal fourth-order term which leads to eq.5 in the text. In eq.S2.3 the polar coordinate representations

$$E_\pm=\frac{1}{2}K_\varepsilon(Q_x^2+Q_y^2)+j(Q_x^2+Q_y^2)^2\pm\frac{g}{2}(Q_x^2+Q_y^2)^2=\frac{1}{2}(K_\varepsilon\pm g)\rho^2+j\rho^4 \qquad \text{(S2.3)}$$

of Q_x and Q_y (eq.6) have been introduced; here ρ is the RT radius (eq. 7), while φ defines the direction of the distortion. Being cyclic, the coordinate φ disappears in the energy expressions (eq.S2.3, last term). Minimization of the ground state energy E_- (eq.S2.3) with respect to ρ yields expressions for ρ_{min}, the stabilization energy E_{RT}, and the energy of the vertical Franck-Condon transition E_{FC} from the lower to the upper sheet of the APES at the position of the minima in terms of the parameters of the model. In the

present work, these parameters were adjusted by utilizing the following expressions:

$$\rho_{\min} = \sqrt{\frac{(g - K_\varepsilon)}{4j}} \qquad g > K_\varepsilon \tag{S2.4}$$

$$E_{RT} = -E_-(\rho = \rho_{\min}) = \frac{1}{16}\frac{(g - K_\varepsilon)^2}{j} \tag{S2.5}$$

$$E_{FC} = E_+(\rho = \rho_{\min}) - E_-(\rho = \rho_{\min}) = g\rho_{\min} = g\frac{(g - K_\varepsilon)}{4j} \tag{S2.6}$$

Temperature-dependent isothermal magnetic susceptibilities and magnetization curves were calculated using a Hamiltonian of the form:

$$\hat{H} = \hat{H}_{vib} + \hat{H}_{SOC} + \hat{H}_{RT} + \hat{H}_Z \tag{S2.7}$$

where, in addition to the Harmonic force term $\hat{H}_{vib}$ (eq.S2.8) the kinetic energy operator $\frac{1}{2}\hbar\omega_\varepsilon(\hat{P}_x^{'2} + \hat{P}_y^{'2})$ has been introduced:

$$\hat{H}_{vib} = \frac{1}{2}\hbar\omega_\varepsilon(\hat{P}_x^{'2} + \hat{P}_y^{'2} + Q_x^{'2} + Q_y^{'2}) \tag{S2.8}$$

Here, $\hbar\omega_\varepsilon$ is the energy of the two-dimensional harmonic oscillator and $\hat{P}_i^{'}$ and $\hat{Q}_i^{'}$ are dimensionless operators related to the observables for momentum and position by:

$$\hat{P}_i^{'} = \frac{1}{\sqrt{\mu\hbar\omega_\varepsilon}}\hat{P}_i; Q_i^{'} = \sqrt{\frac{\mu\omega_\varepsilon}{\hbar}}Q_i; i = x, y \tag{S2.9}$$

The Hamiltonian of eq.S2.7 has been set up in the basis of the products of electronic wavefunctions $|\phi_i\rangle = |M_L = \pm 2, M_S = \pm 2, \pm 1, 0\rangle, i = 1{:}10$ and harmonic vibrational $|\chi_j(Q_x^{'}\rangle . |\chi_k(Q_y^{'}\rangle$ wavefunctions up to level n_{vib}.

$$|\Psi\rangle = \sum_{i=1}^{10} \sum_{j} \sum_{k} \sum_{j+k=0}^{n_{vib}} c_{ijk} \left| \phi_i \chi_j(Q_x^{'}) \chi_k(Q_y^{'}) \right\rangle \qquad \text{(S2.10)}$$

The total basis size N_v, without exploiting symmetries of vibronic wavefunctions, is given by:

$$N_v = 10[\frac{n_{vib}(n_{vib}+1)}{2}] \qquad \text{(S2.11)}$$

With the parameter set j=8.2, g=461 and $\hbar\omega_{\varepsilon} = 131$ cm^{-1}, the five lowest thermally accessible levels are reproduced with good accuracy by taking vibrational levels up n_{vib}=16 into account (corresponding to a $N_v \times N_v$=1360x1360 matrix representation of $\hat{H}$). Isothermal magnetic susceptibilities and magnetizations were calculated employing the representation of $\hat{H}_Z$ in the basis $|\Psi\rangle$ (eq.S2.10) and making explicit use of the calculated eigenvectors following procedures outlined previously.[47]

Vibronic coupling in the presence of static distortions was taken into account following the theory of Ham.[80-81] To this end, an extra term, the strain Hamiltonian H_{Strain} was added to the Hamiltonian of eq.S2.7. We approximate this term with the LF matrix for the 25 quintet states (including the spin variables) deduced from the 1-to-1 mapping of the NEVPT2 results for the quintet states manifold onto ligand field theory:

$$(|M_L=2\rangle|M_L=1\rangle|M_L=0\rangle\ |M_L=-1\rangle\ |M_L=-2\rangle) \otimes \qquad |S=2, M_S=\pm2,\pm1,0\rangle$$

$$H_{Strain} = \begin{bmatrix} -3534 & 325 & 1602 & 304 & 475 \\ 325 & 1196 & 700 & 3162 & 304 \\ 1602 & 700 & 4676 & 700 & 1602 \\ 304 & 3162 & 700 & 1196 & 325 \\ 475 & 304 & 1602 & 325 & -3534 \end{bmatrix} \otimes \begin{bmatrix} 1 & 0 & 0 & 0 & 0 \\ 0 & 1 & 0 & 0 & 0 \\ 0 & 0 & 1 & 0 & 0 \\ 0 & 0 & 0 & 1 & 0 \\ 0 & 0 & 0 & 0 & 1 \end{bmatrix} \qquad \text{(S2.12)}$$

This resulted in the (3400 ×3400) matrix of the Hamiltonian (including the effect of the magnetic field via the matrix of the Zeeman operator) which was solved in the same way as the Hamiltonian from eq.S2.7. In these calculations we have restricted vibronic activity to the ^{5}E ground state and considered vibronic basis functions in the other three excited S=2 states as simple products of electronic and vibrational functions (eq.15).

SI.3. Angular Overlap Model expressions for C_{2v} distorted FeX_2 complexes.

In the angular overlap model the general matrix elements of the 5×5 LF one electron matrix for d-electrons is expressed in terms of parameters defined for well aligned d-orbitals of σ and π-type, e_λ (λ=σ,πc,πs) multiplied by factors $F_{\lambda\omega}(\theta_l,\varphi_l,\psi_l)$ that depend solely on the angular geometry of the ligands (l, described by the Euler angles ($\theta_l,\varphi_l,\psi_l$)).

$$\mathbf{H}^{\mathbf{AOM}}(p_\lambda) = \{H_{ij}^{AOM} = \sum_L \sum_\lambda F_{\lambda i}(\theta_l,\varphi_l,\psi_l) F_{\lambda j}(\theta_l,\varphi_l,\psi_l) e_{\lambda,l}; \lambda = \sigma,\pi c,\pi s\} \qquad \text{(S3.1)}$$

The derived AOM energy expressions for a FeX_2 complex with C_{2v} symmetry (with a choice of Cartesian axes as shown in Figure 3) are given in eqs.S3.2.

$$\begin{array}{lcc} a_1: & |3d_{z2}\rangle & |3d_{x2-y2}\rangle \\ & \begin{bmatrix} (1/8)(1+3\cos 2\theta)^2.e_\sigma + (3/2)\sin^2 2\theta.e_{\pi c} & (\sqrt{3}/4)(1+3\cos 2\theta)\sin^2\theta.e_\sigma - (\sqrt{3}/2)\sin^2 2\theta.e_{\pi c} \\ (\sqrt{3}/4)(1+3\cos 2\theta)\sin^2\theta.e_\sigma - (\sqrt{3}/2)\sin^2 2\theta.e_{\pi c} & (3/2)\sin^4\theta.e_\sigma + (1/2)\sin^2 2\theta.e_{\pi c} \end{bmatrix} \\ a_2: |3d_{yz}\rangle & 2\cos^2\theta e_{\pi s} & \\ b_1: |3d_{xy}\rangle & 2\sin^2\theta e_{\pi s} & \\ b_2: |3d_{xz}\rangle & (3/2)\sin^2 2\theta e_\sigma + 2\cos^2 2\theta e_{\pi c} & \end{array} \qquad \text{(S3.2)}$$

Substitution of θ for a linear FeX_2 complex (Figure 3) leads to eq.10.

SI.4. Pseudo-Jahn-Teller activity due to 3d-4p leading to off-centric distortion in hypothetical (d^5) $FeCl_2^+$ and $Mn(CH_3)_2$.

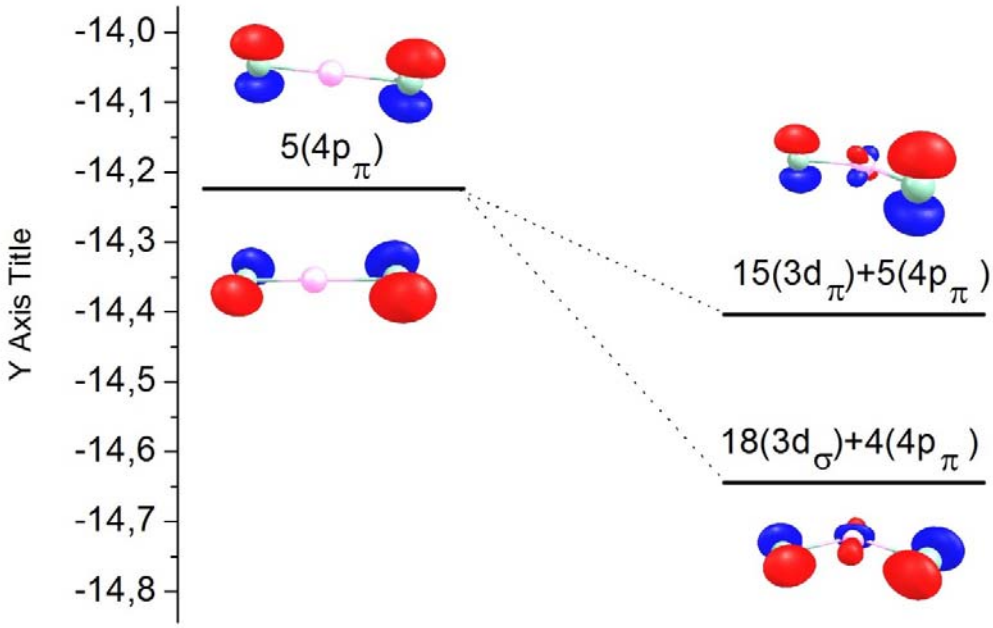

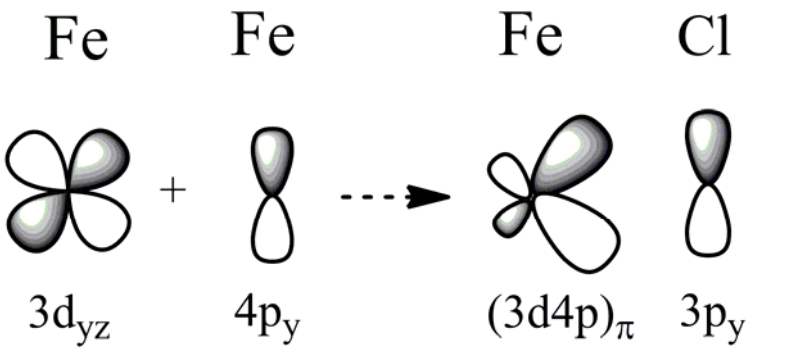

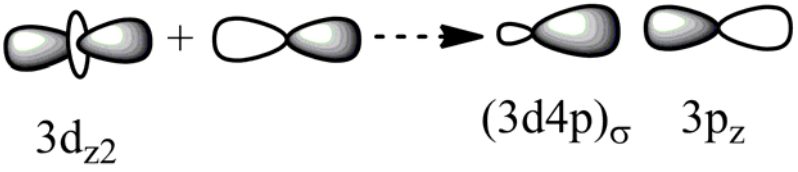

SI.5 Near infrared d-d absorption due to FeN_2 linear core in complex 1

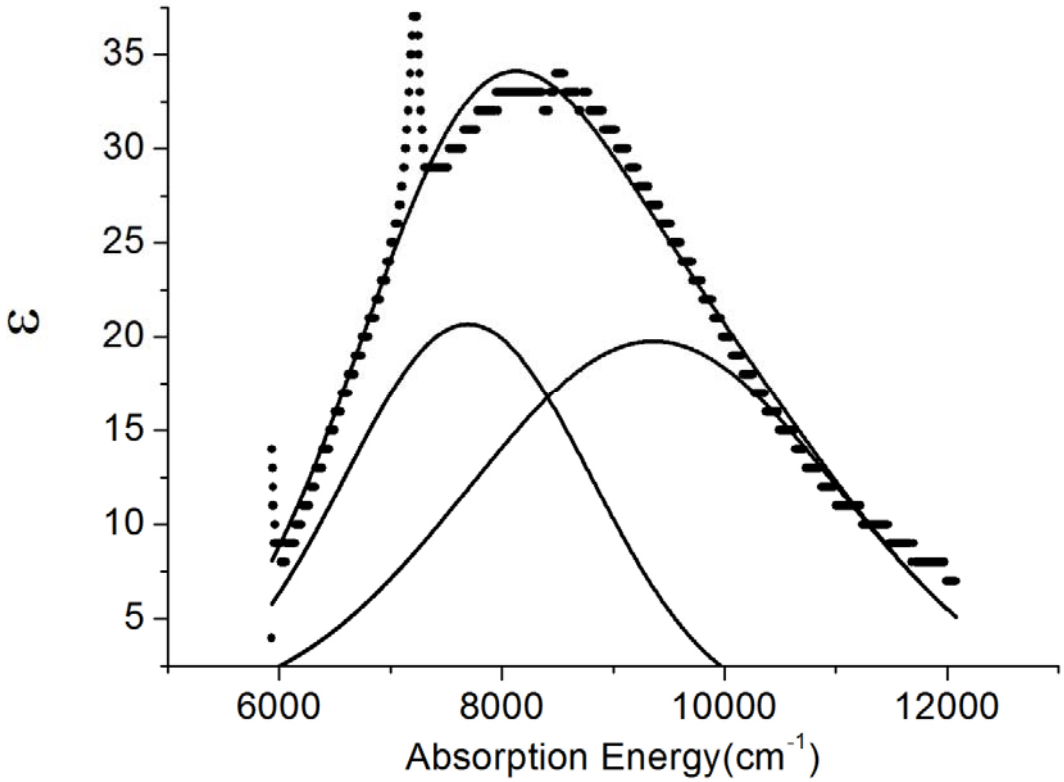

Near infrared d-d absorption due to the FeN_2 linear core in complex **1** (points) and its simulation with two Gaussian envelopes ($F=b_3.\exp\{-[(x-b_1)/b_2]^2\}+ b_6.\exp\{-[(x-b_4)/b_5]^2\}$); b_1=7696 cm^{-1}, b_2=1563 cm^{-1}, b_3=21; b_4=9360 cm^{-1}, b_5=2336 cm^{-1}, b_6=20 and a standard deviation for ε 1.75.

SI.6. Experimental (Ref.55) and *ab initio* (NEVPT2, static geometry from x-ray data) of the molar susceptibility (χT) and molar isothermal magnetization (M) of complex 2.

Experimental (blue squares, from Ref.55) and theoretical (NEVPT2, red circles) magnetic susceptibility of complex **2** in the temperature range from 2K to 300K under a static applied dc field B of 1000 Oe:

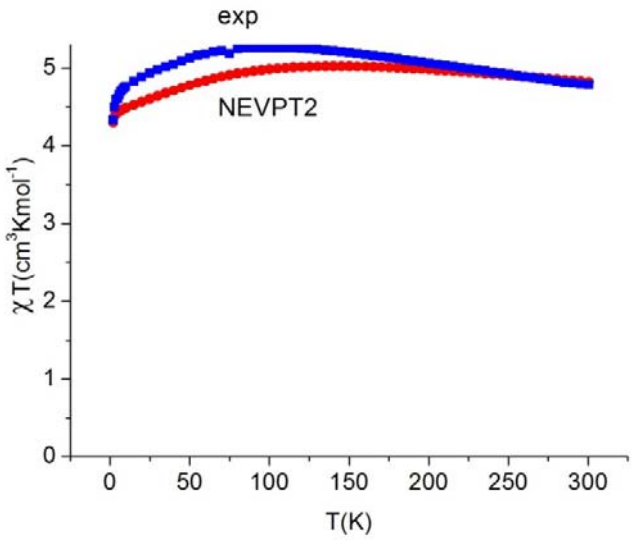

Experimental (Ref.55, red squares, from Ref.55) and calculated (spherical averaged and main values M_z and $M_{x,y}$, NEVPT2, blue squares) magnetization of complex

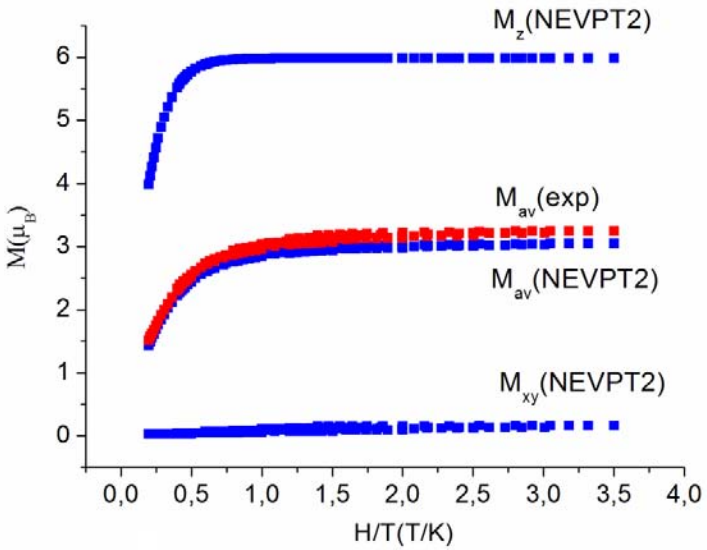

2:

SI.7. Experimental (Ref.55) and *ab initio* (NEVPT2, static geometry from X-ray data) of the molar susceptibility (χT) and molar isothermal magnetization (M) of complexes 3-6.

Experimental (Ref.55, green squares) and theoretical (NEVPT2, blue line) magnetic susceptibility of complex **3** in the temperature range from 2K to 300K under a static applied dc field *B* of 1000 Oe:

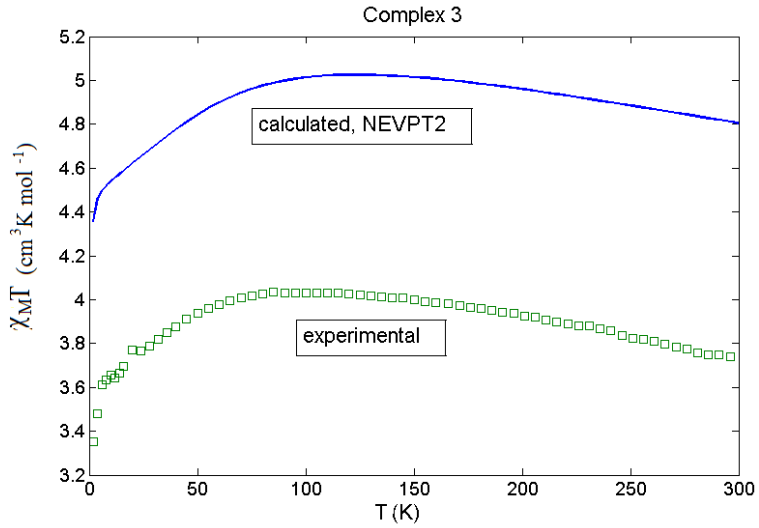

Experimental (Ref.55, green squares) and calculated (NEVPT2, blue stars) magnetization of complex **3**:

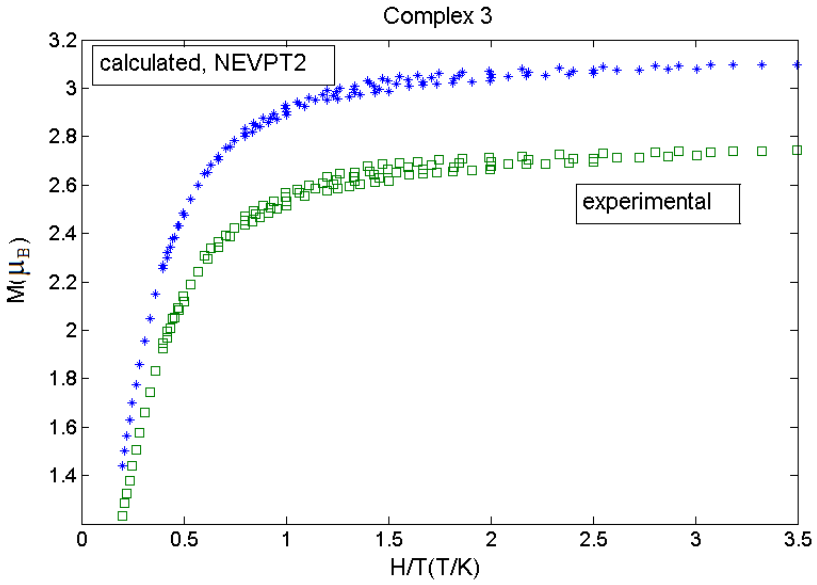

Experimental (Ref.55, green squares) and theoretical (NEVPT2, blue line) magnetic susceptibility of complex **4** in the temperature range from 2K to 300K under a static applied dc field *B* of 1000 Oe:

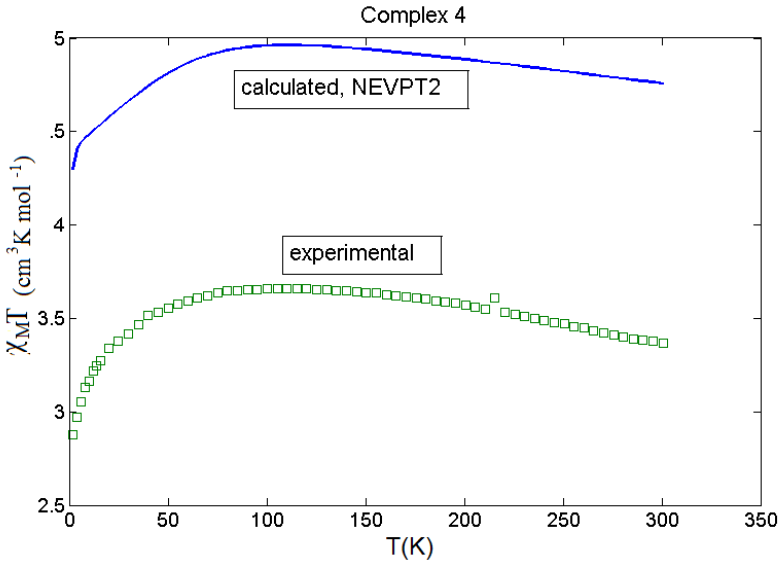

Experimental (Ref.55, green squares) and calculated (NEVPT2, blue stars) magnetization of complex **4**:

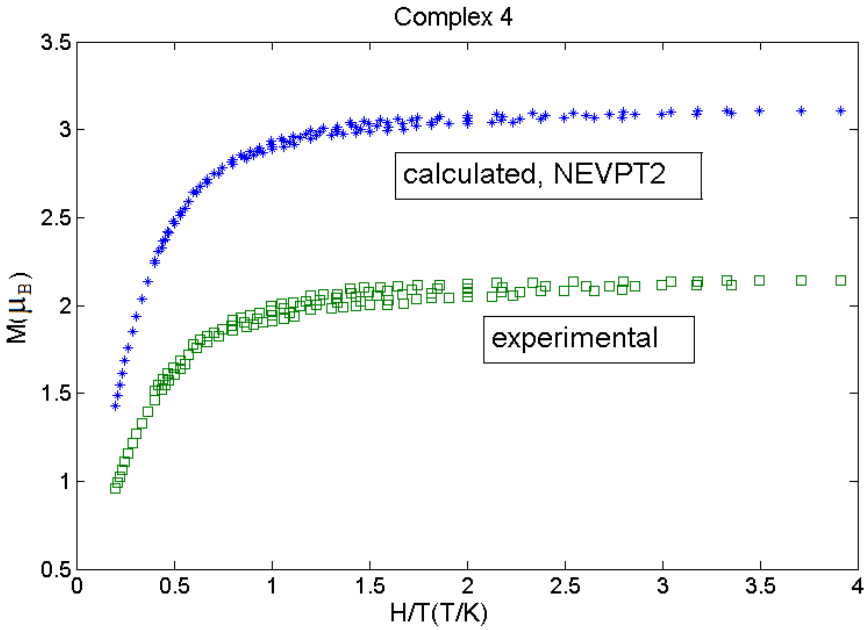

Experimental (Ref.55, green squares) and theoretical (NEVPT2, blue line) magnetic susceptibility of complex **5** in the temperature range from 2K to 300K under a static applied dc field *B* of 1000 Oe:

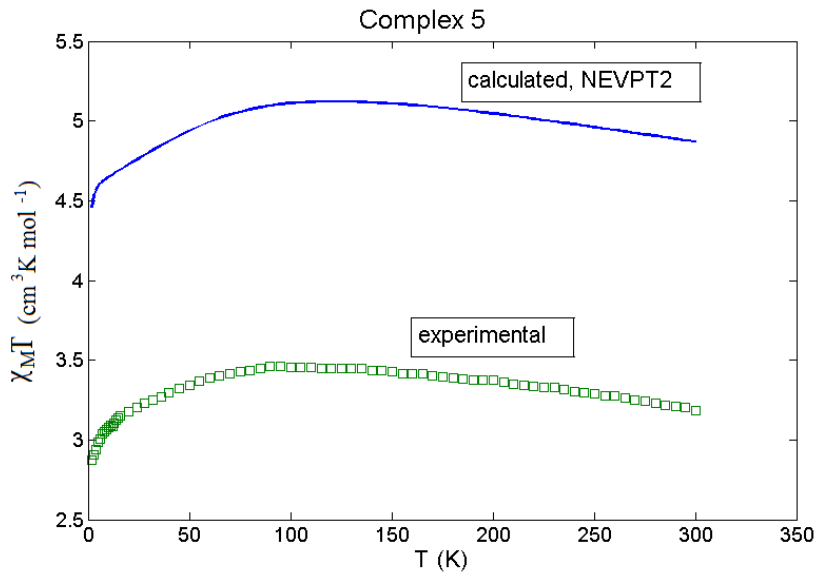

Experimental (Ref.55, green squares) and calculated (NEVPT2, blue stars) magnetization of complex **5**:

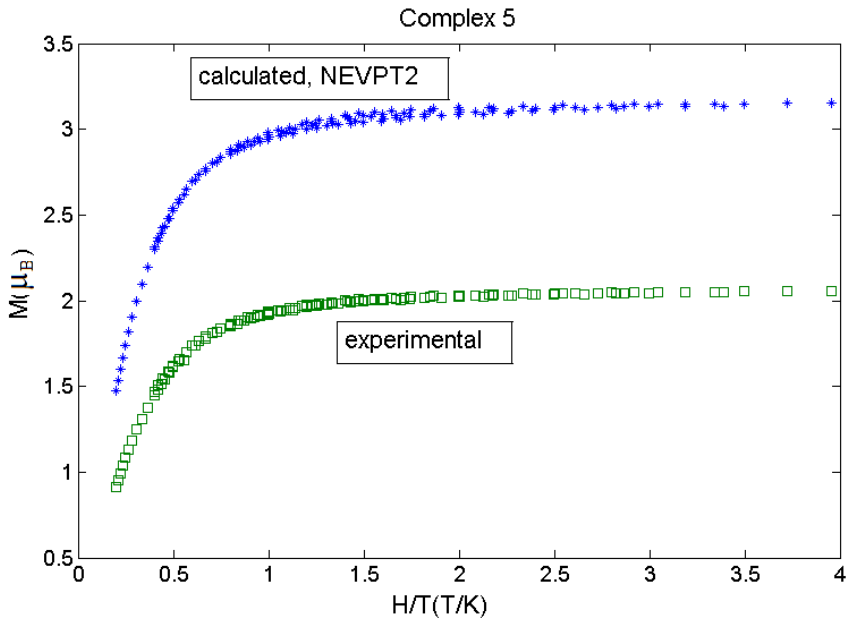

Experimental (Ref.55, green squares) and theoretical (NEVPT2, blue line) magnetic susceptibility of complex **6** in the temperature range from 2K to 300K under a static applied dc field *B* of 1000 Oe:

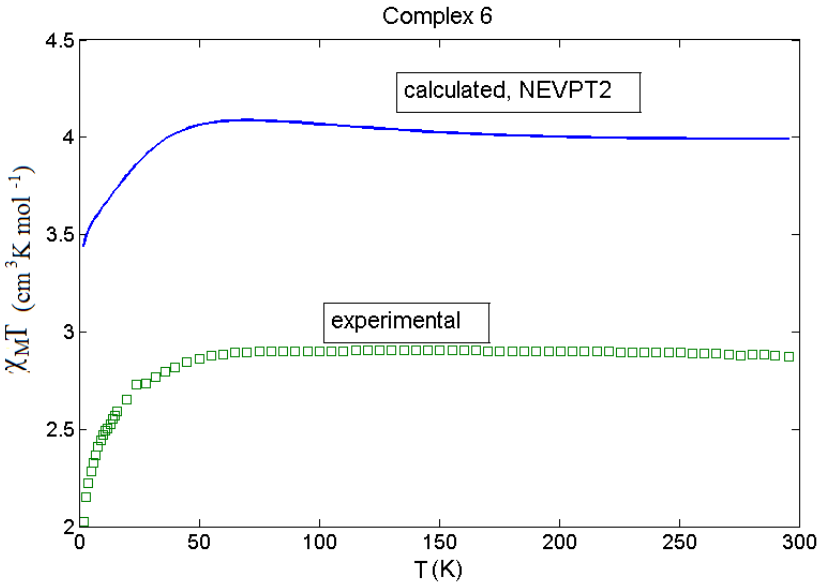

Experimental (Ref.55, green squares) and calculated (NEVPT2, blue stars) magnetization of complex **6**:

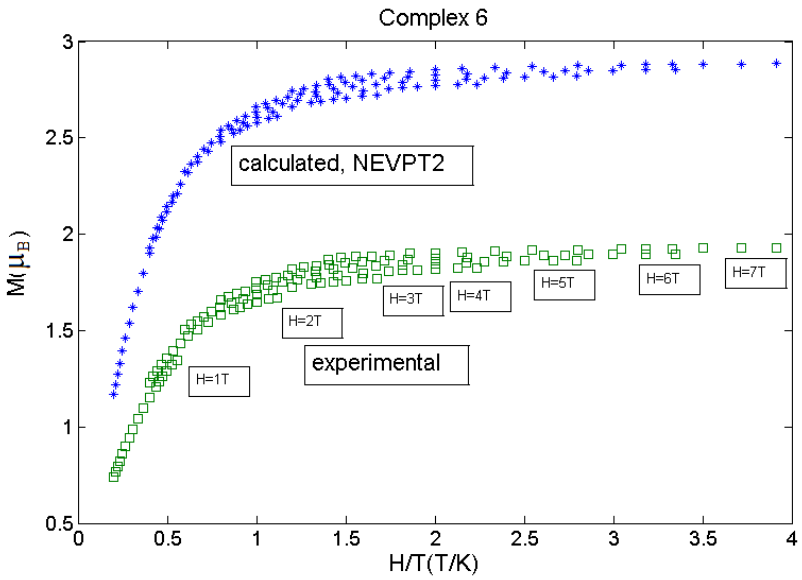

SI.8 Effect of the Stevens orbital reduction factor k introduced into the Zeeman operator $H_z=\beta H(2S+kL)$ on the magnetic susceptibility (top) and the isothermal magnetization for complex 3 (bottom)

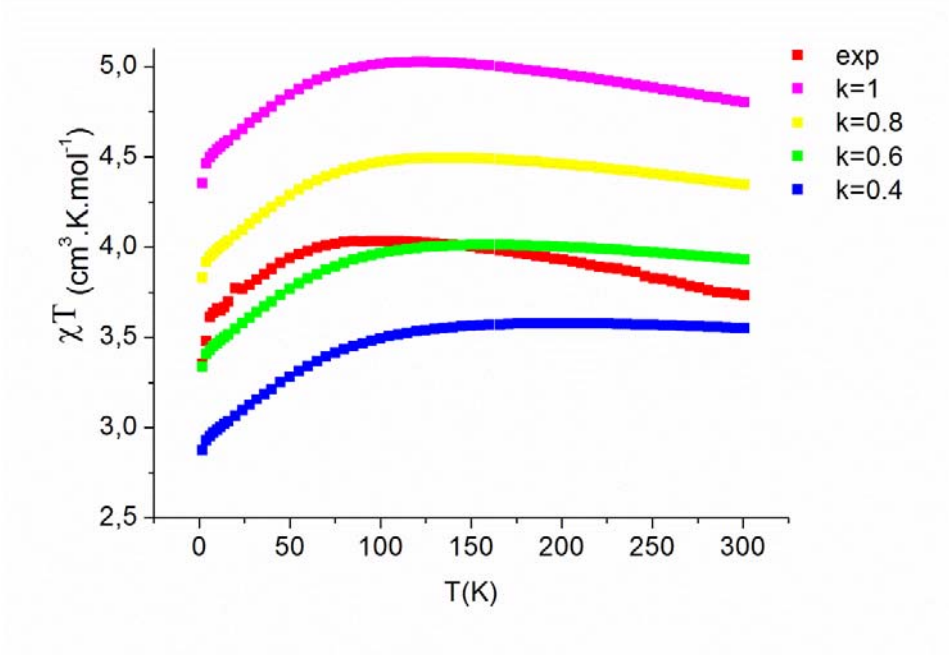

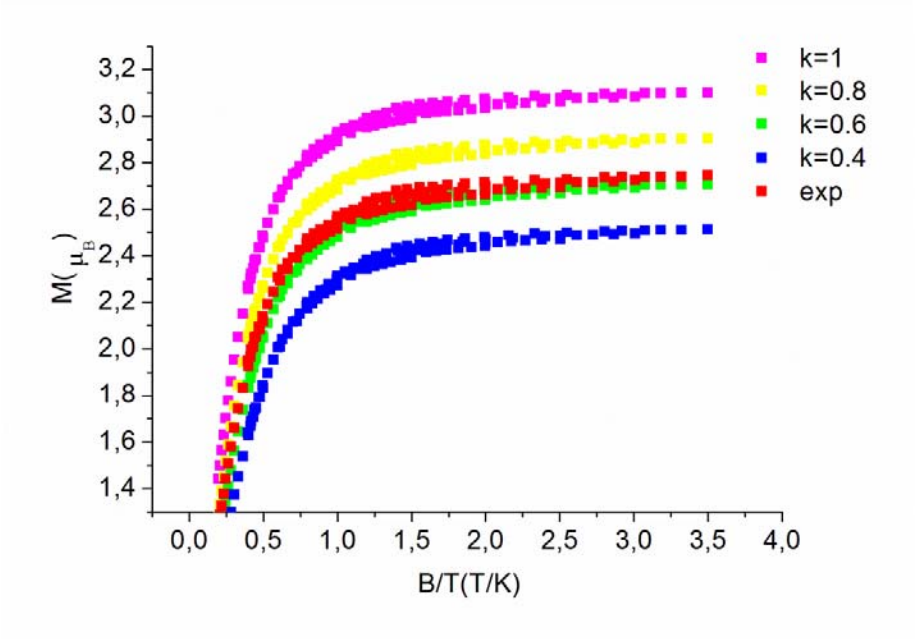

SI.9 Vibronic energy level diagrams for the limiting case of zero vibronic coupling *f*=0, static limit and *f*=0.1

Combined electronic - vibrational energy level diagram for the limiting case of zero vibronic coupling *f*=0, static limit, (a) and *f*=0.1

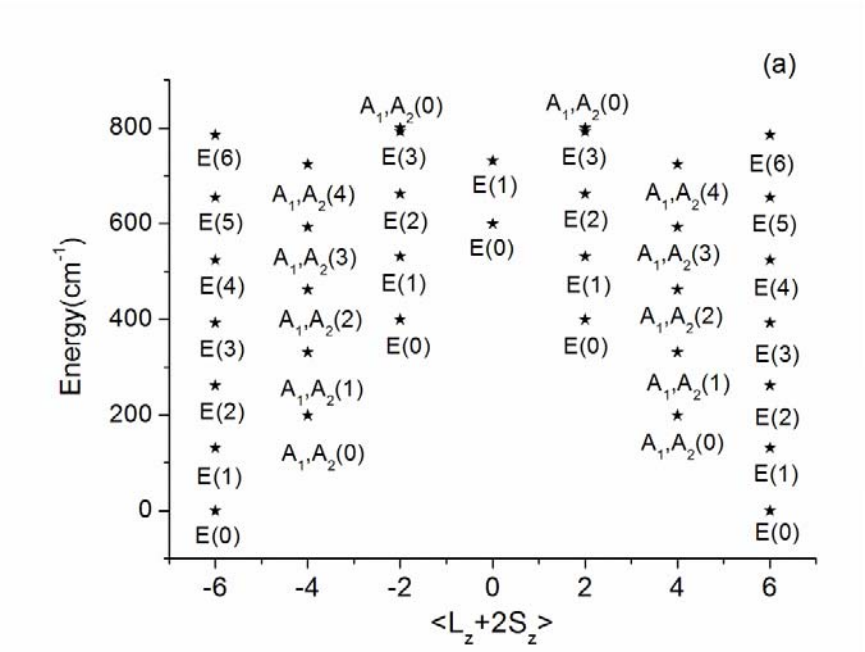

(b):

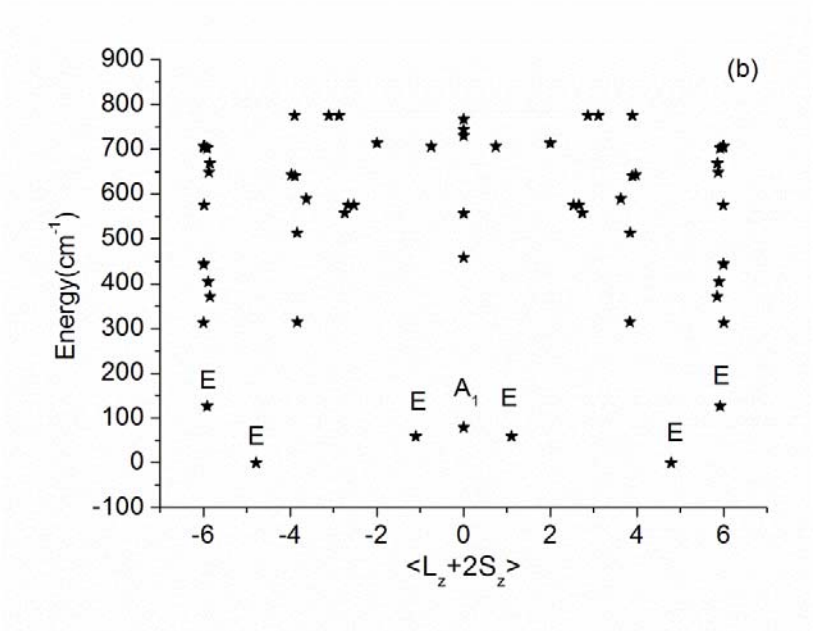

SI.10 Vibronically driven mixing between $|M_L=2, M_S=2\rangle$ and $|M_L=-2, M_S=2\rangle$ total angular momentum states (top) and large amplitude motions (bottom):

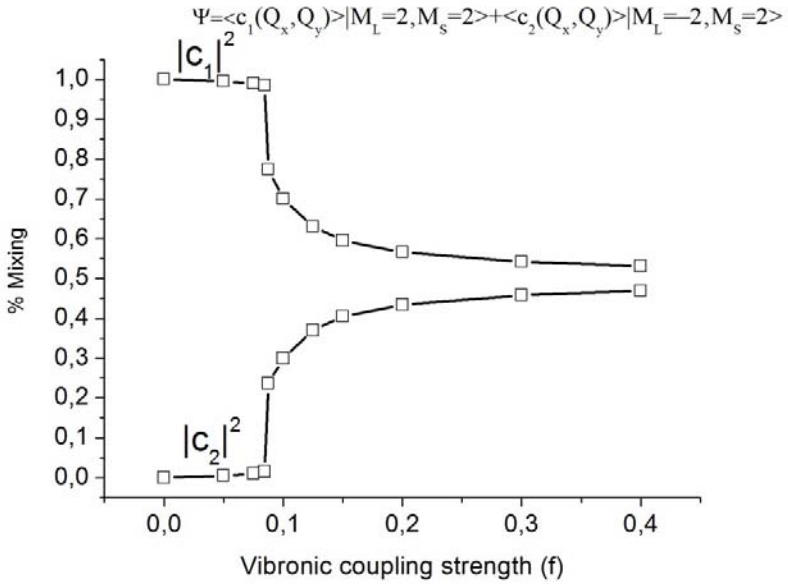

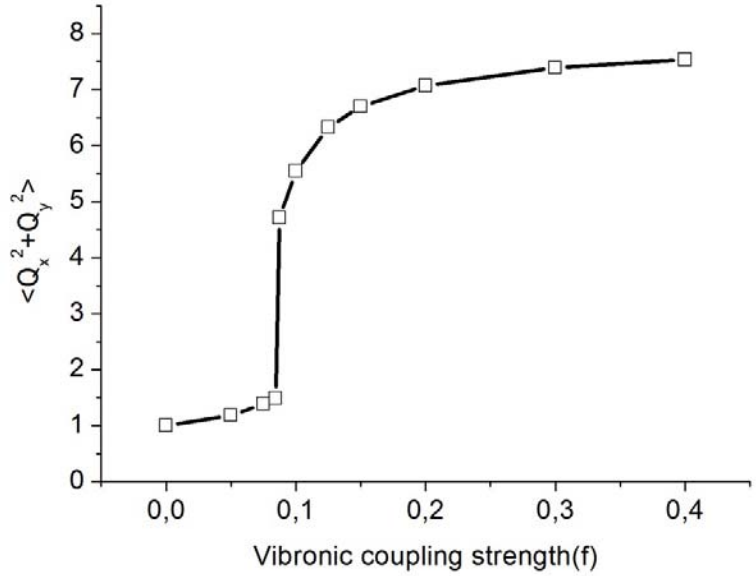

SI.11. Dependence of the magnetization on the vibronic coupling strength *f*.

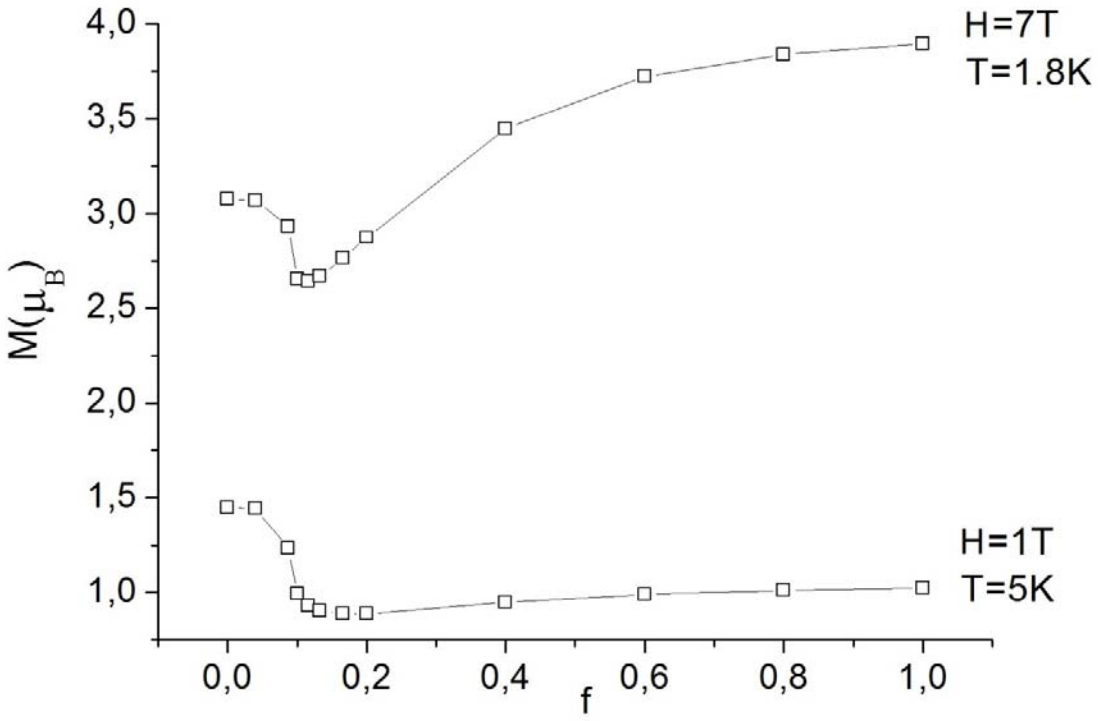

SI.12. Variations of the Lewis basicity with the ligand substituents.

The affinity of OH^-, NH_2^- and CH_3^-, toward the proton as quantified by the energy E_B defined in the figure below reflects the expected increase of the Lewis basicity of these anions across this series. For comparison in this figure we also include the corresponding values of E_B for the ligand of complexes **1-7**. The comparison reflects a dramatic change of the Lewis basicity –an overall decrease with respect to the CH_3^-, NH_2^- and OH^- and additionally variations with the substituents (for the N-ligands).

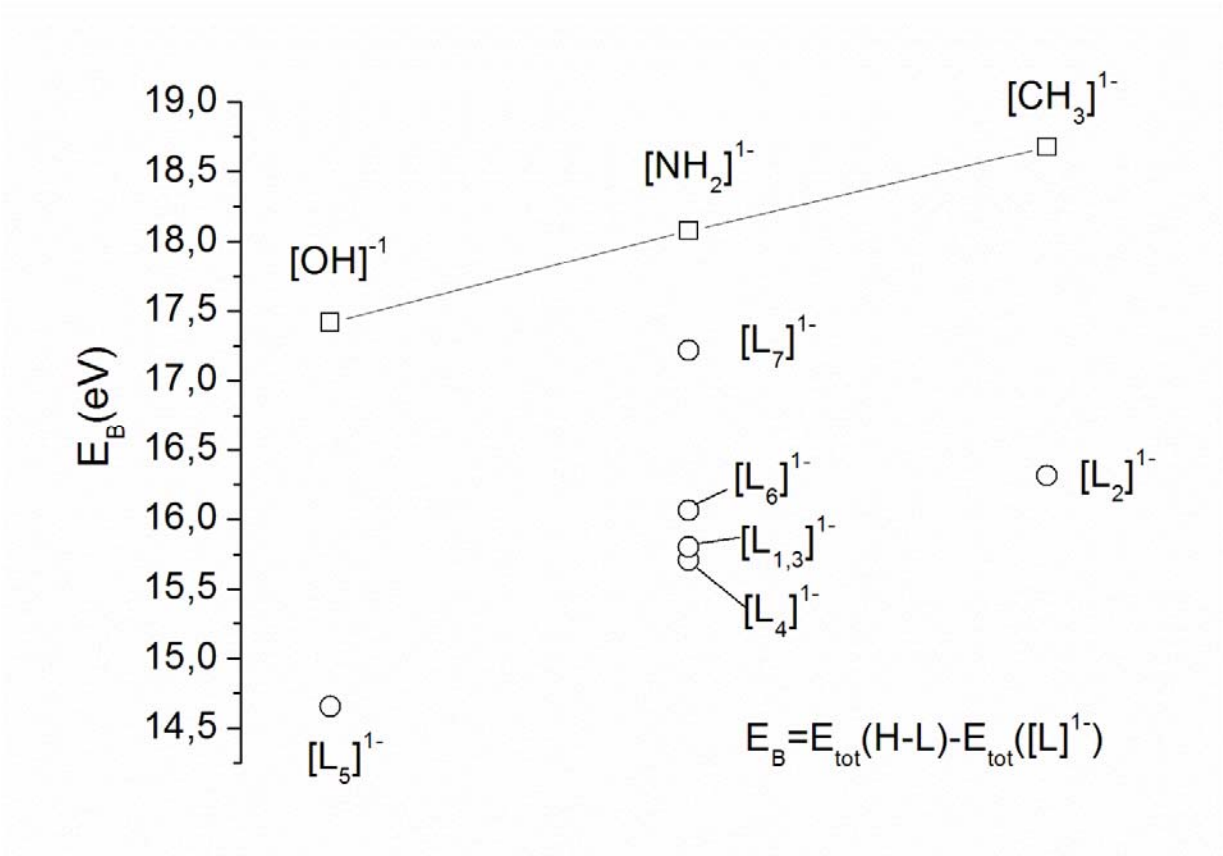

SI.13. Complete list of LF matrices $\mathbf{H}^{\mathbf{LFT}}_{\mathbf{NEVPT2}}(S=2, M_s=2)$ for complexes 1-6 from a 1-to-1 mapping to NEVPT2 results

LF matrices for the S=2, M_S=2 states:

Complex 1

$$\mathbf{H}^{\mathbf{LFT}}_{\mathbf{NEVPT2}}(S=2, M_s=2) = \begin{array}{c} \begin{matrix} |d_{z2}> & |d_{xz}> & |d_{yz}> & |d_{x2-y2}> & |d_{xy}> \end{matrix} \\ \begin{bmatrix} 2576 & -532 & -34 & 270 & 829 \\ -532 & -471 & -156 & 36 & -255 \\ -34 & -156 & 6147 & 44 & -563 \\ 270 & 36 & 44 & -4155 & 102 \\ 829 & -255 & -563 & 102 & -4097 \end{bmatrix} \end{array}$$

Complex 2

$$\mathbf{H}^{\mathbf{LFT}}_{\mathbf{NEVPT2}}(S=2, M_s=2) = \begin{array}{c} \begin{matrix} |d_{z2}> & |d_{xz}> & |d_{yz}> & |d_{x2-y2}> & |d_{xy}> \end{matrix} \\ \begin{bmatrix} 2130 & -43 & -4 & -9 & -116 \\ -43 & 1852 & 15 & 45 & 64 \\ -4 & 15 & 1810 & 24 & -177 \\ -9 & 45 & 24 & -2868 & 32 \\ -116 & 64 & -177 & 32 & -2924 \end{bmatrix} \end{array}$$

Complex 3

$$\mathbf{H}^{\mathbf{LFT}}_{\mathbf{NEVPT2}}(S=2, M_s=2) = \begin{array}{c} \begin{matrix} |d_{z2}> & |d_{xz}> & |d_{yz}> & |d_{x2-y2}> & |d_{xy}> \end{matrix} \\ \begin{bmatrix} 5107 & -137 & -4 & -897 & 690 \\ -137 & -1865 & 121 & 171 & -96 \\ -4 & 121 & 4217 & 36 & 169 \\ -897 & 171 & 36 & -3650 & -183 \\ 690 & -96 & 169 & -183 & -3809 \end{bmatrix} \end{array}$$

Complex 4

$$\mathbf{H}^{\mathbf{LFT}}_{\mathbf{NEVPT2}}(S=2, M_s=2) = \begin{array}{c} \begin{matrix} |d_{z2}\rangle & |d_{xz}\rangle & |d_{yz}\rangle & |d_{x2-y2}\rangle & |d_{xy}\rangle \end{matrix} \\ \begin{bmatrix} 5267 & -111 & 29 & -1518 & -290 \\ -111 & -1720 & 154 & 178 & -3 \\ 29 & 154 & 3965 & 9 & 121 \\ -1518 & 178 & 9 & -3469 & 156 \\ -290 & -3 & 121 & 156 & -4042 \end{bmatrix} \end{array}$$

Complex 5

$$\mathbf{H}^{\mathbf{LFT}}_{\mathbf{NEVPT2}}(S=2, M_s=2) = \begin{array}{c} \begin{matrix} |d_{z2}\rangle & |d_{xz}\rangle & |d_{yz}\rangle & |d_{x2-y2}\rangle & |d_{xy}\rangle \end{matrix} \\ \begin{bmatrix} 6073 & 423 & 3 & -1320 & -836 \\ 423 & 442 & 432 & 153 & 90 \\ 3 & 432 & 2357 & 40 & 138 \\ -1320 & 153 & 40 & -4366 & 220 \\ -836 & 90 & 138 & 220 & -4506 \end{bmatrix} \end{array}$$

Complex 6

$$\mathbf{H}^{\mathbf{LFT}}_{\mathbf{NEVPT2}}(S=2, M_s=2) = \begin{array}{c} \begin{matrix} |d_{z2}\rangle & |d_{xz}\rangle & |d_{yz}\rangle & |d_{x2-y2}\rangle & |d_{xy}\rangle \end{matrix} \\ \begin{bmatrix} 4676 & -84 & -987 & 967 & -2049 \\ -84 & 4358 & -80 & 13 & 296 \\ -987 & -80 & -1965 & -20 & 554 \\ 967 & 13 & -20 & -3105 & -203 \\ -2049 & 296 & 554 & -203 & -3964 \end{bmatrix} \end{array}$$

Matrices $\mathbf{H}^{\mathbf{LFT}}_{\mathbf{NEVPT2}}(S=2, M_s=2)$ have been written down in a form which allows a direct comparison with the corresponding AOM matrices (see SI.3). The former have been transformed into the basis the angular momentum eigenfunctions for $|L, M_L\rangle$, L=2, M_L=±2, ±1, 0 given by the transformation matrix **T**

$$\begin{bmatrix} |2,2\rangle \\ |2,1\rangle \\ |2,0\rangle \\ |2,-1\rangle \\ |2,-2\rangle \end{bmatrix} = \begin{bmatrix} 0 & 0 & 0 & \frac{1}{\sqrt{2}} & \frac{1}{i\sqrt{2}} \\ 0 & -\frac{1}{\sqrt{2}} & \frac{i}{\sqrt{2}} & 0 & 0 \\ 1 & 0 & 0 & 0 & 0 \\ 0 & \frac{1}{\sqrt{2}} & \frac{i}{\sqrt{2}} & 0 & 0 \\ 0 & 0 & 0 & \frac{1}{\sqrt{2}} & -\frac{1}{i\sqrt{2}} \end{bmatrix} \begin{bmatrix} |d_{z2}\rangle \\ |d_{xz}\rangle \\ |d_{yz}\rangle \\ |d_{x2-y2}\rangle \\ |d_{xy}\rangle \end{bmatrix}$$

We identify these transformed matrices with the Strain energy Hamiltonian employed in calculations of vibronic levels in the presence of low-symmetry ligand field strain:

$$\mathbf{H}_{\mathbf{Strain}} = \mathbf{T}\mathbf{H}^{\mathbf{LFT}}_{\mathbf{NEVPT2}}\mathbf{T}^{\dagger}$$

The matrices $\mathbf{H}_{\mathbf{Strain}}$ are complex. Below we list the diagonal elements and the moduli $\sqrt{H_{Strain}(i,j).H^{*}_{Strain}(i,j)}$ of the off-diagonal $H_{Strain}(i,j)$, i≠j:

Complex 1

$$\mathbf{H}_{\mathbf{Strain}} = \begin{array}{c} \begin{matrix} |2,2> & |2,1> & |2,0> & |2,-1> & |2,-2> \end{matrix} \\ \begin{bmatrix} -4126 & 303 & 616 & 318 & 106 \\ 303 & 2838 & 377 & 3313 & 318 \\ 616 & 377 & 2576 & 377 & 616 \\ 318 & 3313 & 377 & 2838 & 303 \\ 106 & 318 & 616 & 303 & -4126 \end{bmatrix} \end{array}$$

Complex 2

$$\mathbf{H}_{\mathbf{Strain}} = \begin{array}{c} \begin{matrix} |2,2> & |2,1> & |2,0> & |2,-1> & |2,-2> \end{matrix} \\ \begin{bmatrix} -2896 & 69 & 82 & 119 & 43 \\ 69 & 1831 & 30 & 26 & 119 \\ 82 & 30 & 2130 & 30 & 82 \\ 119 & 26 & 30 & 1831 & 69 \\ 43 & 119 & 82 & 69 & -2896 \end{bmatrix} \end{array}$$

Complex 3

$$\mathbf{H}_{\mathbf{Strain}} = \begin{array}{c} \begin{matrix} |2,2\rangle & |2,1\rangle & |2,0\rangle & |2,-1\rangle & |2,-2\rangle \end{matrix} \\ \begin{bmatrix} -3730 & 182 & 800 & 30 & 199 \\ 182 & 1176 & 97 & 3043 & 30 \\ 800 & 97 & 5107 & 97 & 800 \\ 30 & 3043 & 97 & 1176 & 182 \\ 199 & 30 & 800 & 182 & -3730 \end{bmatrix} \end{array}$$

Complex 4

$$\mathbf{H}_{\mathbf{Strain}} = \begin{array}{c} \begin{matrix} |2,2\rangle & |2,1\rangle & |2,0\rangle & |2,-1\rangle & |2,-2\rangle \end{matrix} \\ \begin{bmatrix} -3756 & 149 & 1093 & 29 & 326 \\ 149 & 1122 & 81 & 2846 & 29 \\ 1093 & 81 & 5267 & 81 & 1093 \\ 29 & 2846 & 81 & 1122 & 149 \\ 326 & 29 & 1093 & 149 & -3756 \end{bmatrix} \end{array}$$

Complex 5

$$\mathbf{H}_{\mathbf{Strain}} = \begin{array}{c} \begin{matrix} |2,2\rangle & |2,1\rangle & |2,0\rangle & |2,-1\rangle & |2,-2\rangle \end{matrix} \\ \begin{bmatrix} -4436 & 147 & 1105 & 66 & 231 \\ 147 & 1400 & 299 & 1051 & 66 \\ 1105 & 299 & 6073 & 299 & 1105 \\ 66 & 1051 & 299 & 1400 & 147 \\ 231 & 66 & 1105 & 147 & -4436 \end{bmatrix} \end{array}$$

Complex 6

$$\mathbf{H}_{\mathbf{Strain}} = \begin{array}{c} \begin{matrix} |2,2\rangle & |2,1\rangle & |2,0\rangle & |2,-1\rangle & |2,-2\rangle \end{matrix} \\ \begin{bmatrix} -3535 & 324 & 1602 & 304 & 475 \\ 324 & 1197 & 700 & 3162 & 304 \\ 1602 & 700 & 4676 & 700 & 1602 \\ 304 & 3162 & 700 & 1197 & 324 \\ 475 & 304 & 1602 & 324 & -3535 \end{bmatrix} \end{array}$$

Matrix elements expressed in the $|L, M_L\rangle$, L=2, M_L=±2, ±1, 0 basis are particularly suitable for an analysis of the effect of low-symmetry ligand field on the orbital moment reduction. Below we plot some matrix elements of relevance for the discussion in Section 3.2.3.

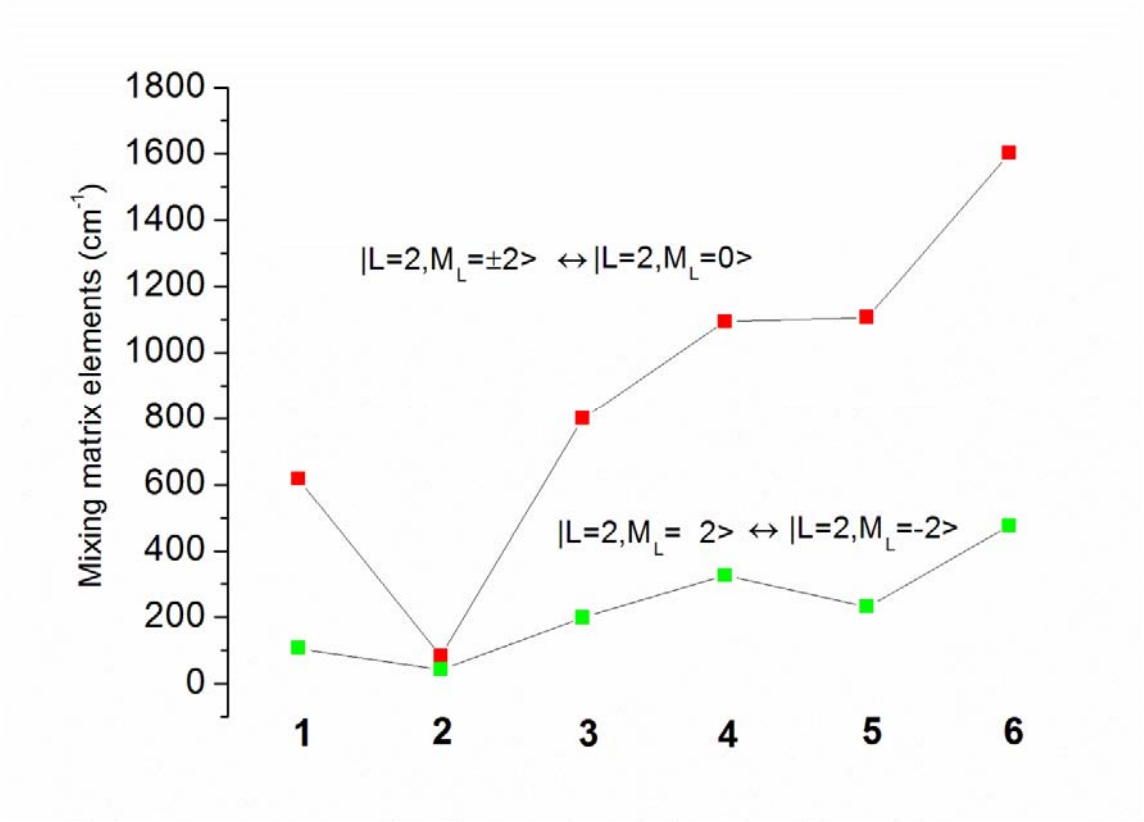

Matrix elements affecting the orbital moments of the magnetic ground states of the $Fe^{II}X_2$ SMM, responsible for the orbital moment reduction and quantum tunneling of the magnetization.

SI.14 Energies of the lowest ground state quintet to the lowest eleven triplet transitions from NEVPT2 and the spin-orbit split terms from the nominal ^{5}E ground state calculated using full CI within the manifold of the electronic states due to the d^6 configuration of Fe(II) and deductions of *B*, *C* and ζ from a best fit to these data.

FeN2, Complex 1; B and C from a least squares fit to spin-forbidden transitions

	energy (NEVPT2)	energy(calc.)	difference	weight
31	18023.000	16942.277	-1080.723	1.000
31	18145.000	16967.543	-1177.457	1.000
31	19390.000	17898.579	-1491.421	1.000
31	20209.000	19504.469	-704.531	1.000
31	20328.000	20006.306	-321.694	1.000
31	20394.000	20747.511	353.511	1.000
31	20403.000	20770.940	367.940	1.000
31	20655.000	20883.799	228.799	1.000
31	20657.000	21413.907	756.907	1.000
31	21403.000	22556.880	1153.880	1.000
31	21421.000	23334.156	1913.156	1.000

Sigma, weighted = 1011.559

NEXT CALCULATION WITH OPTIMIZED PARAMETERS (AOM parameters from spin quintet transitions)

B = 1511.824021
C = 3245.444663
*
esig = 3351.000000
epis = 5137.000000
epic = 1828.000000

AOM matrix

xy	xz	yz	x2y2	z2
.000	.000	.000	.000	.000
.000	3656.000	.000	.000	.000
.000	.000	10274.000	.000	.000
.000	.000	.000	.000	.000
.000	.000	.000	.000	6702.000

zeta from a least squares fit to SOC split terms of ^{5}E:

NEXT CALCULATION WITH OPTIMIZED PARAMETERS

zeta = 413.702538
*
esig = 3351.000000
epis = 5137.000000
epic = 1828.000000
B = 1512.000000
C = 3245.000000

```
  2        .000             2
  4     204.681             2
  5     408.099             1
  6     408.252             1
  7     605.394             1
  8     616.113             1
  9     812.321             1
 10     812.631             1



          energy (NEVPT2)   energy(calc.)  difference    weight

2A             189.8,190.4         204.681      14.681     1.000
1A              322.800          408.099      85.299     1.000
1A              485.500          408.252     -77.248     1.000
1A              612.800          605.394      -7.406     1.000
1A              625.000          616.113      -8.887     1.000
1A              810.100          812.321       2.221     1.000
1A              810.300          812.631       2.331     1.000

Sigma, weighted =       44.082
```

FeC2, Complex 2 ; B and C from a least squares fit to spin-forbidden transitions

```
NEXT CALCULATION WITH OPTIMIZED PARAMETERS

B          =   1418.171058
C          =   3563.521806
*
esig       =   2513.000000
epis       =   2364.000000
epic       =   2364.000000

AOM matrix

        xy        xz        yz      x2y2        z2

      .000      .000      .000      .000      .000
      .000  4728.000      .000      .000      .000
      .000      .000  4728.000      .000      .000
      .000      .000      .000      .000      .000
      .000      .000      .000      .000  5026.000


    energy (NEVPT2)           energy(calc.)  difference    weight

32        21255.6,21320.2       21165.877    -122.123     1.000
32        21363.6,21475.4       21386.612     -33.388     1.000
32        21846.2, 21901.7      21408.693    -465.307     1.000
31        20622.500         21467.156     845.156     1.000
32        22185.5, 22201.5      22070.948    -123.052     1.000
32        23454.5, 23458.5      23361.753     -94.247     1.000



Sigma, weighted =      402.254

NEXT CALCULATION WITH OPTIMIZED PARAMETERS

zeta       =    407.038120
*
esig       =   2513.000000
epis       =   2364.000000
epic       =   2364.000000
B          =   1418.000000
C          =   3564.000000
```

	energy(NEVPT2)	energy(calc.)	difference	weight
2	195.2,195.3	200.043	4.843	1.000
2	353.0,444.6	400.051	1.051	1.000
2	602.0,603.8	600.084	-2.816	1.000
1	799.7	800.026	.026	1.000
1	800.0	800.350	.350	1.000

Sigma, weighted = 2.554

FeN2 Complex 3

NEXT CALCULATION WITH OPTIMIZED PARAMETERS

B = 970.316709
C = 3781.851172
*
esig = 4418.000000
epis = 3973.000000
epic = 932.000000

AOM matrix

xy	xz	yz	x2y2	z2
.000	.000	.000	.000	.000
.000	1864.000	.000	.000	.000
.000	.000	7946.000	.000	.000
.000	.000	.000	.000	.000
.000	.000	.000	.000	8836.000

	energy (exp.)	energy(calc.)	difference	weight
31	14944.000	16992.330	2048.330	1.000
31	15300.000	17364.524	2064.524	1.000
31	18596.000	17714.038	-881.962	1.000
31	19868.000	19209.173	-658.827	1.000
31	20031.000	19357.001	-673.999	1.000
31	20408.000	19957.752	-450.248	1.000
31	20545.000	20421.458	-123.542	1.000
31	20832.000	20422.267	-409.733	1.000
31	21284.000	20593.476	-690.524	1.000
31	21911.000	21682.768	-228.232	1.000
31	21928.000	21771.679	-156.321	1.000

Sigma, weighted = 1002.874

NEXT CALCULATION WITH OPTIMIZED PARAMETERS

zeta = 426.569658
*
esig = 4418.000000
epis = 3973.000000
epic = 932.000000
B = 970.000000
C = 3782.000000

AOM matrix

xy	xz	yz	x2y2	z2
.000	.000	.000	.000	.000
.000	1864.000	.000	.000	.000
.000	.000	7946.000	.000	.000
.000	.000	.000	.000	.000
.000	.000	.000	.000	8836.000

```
no.     Energy   Mult.(total)   Mult.(Spin)   Mult.(Bahn)

  2        .000             2
  4     204.419             2
  5     410.245             1
  6     410.470             1
  7     604.452             1
  8     634.552             1
  9     831.912             1
 10     832.531             1


            energy(NEVPT2)   energy(calc.)  difference    weight

2A          176.400,179.8         204.419      26.319     1.000
1A              286.600         410.245     123.645     1.000
1A              529.100         410.470    -118.630     1.000
1A              632.000         604.452     -27.548     1.000
1A              646.600         634.552     -12.048     1.000
1A              822.000         831.912       9.912     1.000
1A              822.500         832.531      10.031     1.000

Sigma, weighted =       66.715
```

Complex 4

```
NEXT CALCULATION WITH OPTIMIZED PARAMETERS

B          =    822.514678
C          =   3965.134070
*
esig       =   4512.000000
epis       =   3860.000000
epic       =   1018.000000

AOM matrix

        xy        xz        yz      x2y2        z2

      .000      .000      .000      .000      .000
      .000  2036.000      .000      .000      .000
      .000      .000  7720.000      .000      .000
      .000      .000      .000      .000      .000
      .000      .000      .000      .000  9024.000


             energy(NEVPT2)  energy(calc.)  difference    weight

31             14826.000       17026.612    2200.612     1.000
31             15126.000       17320.869    2194.869     1.000
31             18603.000       18005.480    -597.520     1.000
31             19760.000       19276.012    -483.988     1.000
31             20157.000       19493.578    -663.422     1.000
31             20350.000       19899.430    -450.570     1.000
31             20588.000       20435.931    -152.069     1.000
31             21092.000       20439.872    -652.128     1.000
31             21699.000       20624.046   -1074.954     1.000
31             22026.000       21729.541    -296.459     1.000
31             22147.000       21919.030    -227.970     1.000

Sigma, weighted =     1071.886
```

```
NEXT CALCULATION WITH OPTIMIZED PARAMETERS

zeta       =    459.340093
*
esig       =   4512.000000
epis       =   3860.000000
epic       =   1018.000000
B          =    822.000000
C          =   3965.000000


  2        .000            2
  4     220.022            2
  5     441.667            1
  6     441.872            1
  7     651.568            1
  8     682.310            1
  9     895.606            1
 10     896.336            1


             energy(NEVPT2)   energy(calc.)  difference    weight

1A              242.700         441.667     198.967     1.000
1A              624.600         441.872    -182.728     1.000
1A              704.400         651.568     -52.832     1.000
1A              710.100         682.310     -27.790     1.000
1A              870.400         895.606      25.206     1.000
1A              870.700         896.336      25.636     1.000

Sigma, weighted =      113.896
```

FeO2 Complex 5

```
NEXT CALCULATION WITH OPTIMIZED PARAMETERS

B          =   1089.634044
C          =   3734.199544
*
esig       =   5255.000000
epis       =   3397.000000
epic       =   2439.000000

AOM matrix

        xy        xz        yz      x2y2        z2

      .000      .000      .000      .000      .000
      .000  4878.000      .000      .000      .000
      .000      .000  6794.000      .000      .000
      .000      .000      .000      .000      .000
      .000      .000      .000      .000 10510.000
```

```
            energy(NEVPT2)    energy(calc.)  difference    weight

31            16813.000       18701.652    1888.652     1.000
31            17024.000       18752.620    1728.620     1.000
31            19213.000       19697.928     484.928     1.000
31            20376.000       20160.790    -215.210     1.000
31            21559.000       20530.490   -1028.510     1.000
31            21573.000       20896.217    -676.783     1.000
31            21789.000       20898.006    -890.994     1.000
31            21977.000       21615.522    -361.478     1.000
31            22434.000       21653.316    -780.684     1.000
31            22699.000       22438.641    -260.359     1.000
31            23231.000       23146.061     -84.939     1.000

Sigma, weighted =      951.624

EXT CALCULATION WITH OPTIMIZED PARAMETERS

zeta       =    419.695627
*
esig       =   5255.000000
epis       =   3397.000000
epic       =   2439.000000
B          =   1090.000000
C          =   3734.000000

  2        .000            2
  4     207.865            2
  5     414.973            1
  6     414.981            1
  7     619.609            1
  8     623.310            1
  9     827.308            1
 10     827.546            1


             energy(NEVPT2)   energy(calc.)  difference    weight

2A             184.800         207.865      23.065     1.000
1A             300.900         414.973     114.073     1.000
1A             521.400         414.981    -106.419     1.000
1A             632.800         619.609     -13.191     1.000
1A             641.500         623.310     -18.190     1.000
1A             820.400         827.308       6.908     1.000
1A             820.500         827.546       7.046     1.000

Sigma, weighted =       60.323
```

FeN2 Complex 6, bent

```
NEXT CALCULATION WITH OPTIMIZED PARAMETERS

B          =    601.565204
C          =   4363.667501
*
esig       =   5291.000000
epis       =   3414.000000
epic       =    884.000000
```

AOM matrix

xy	xz	yz	x2y2	z2
230.757	299.910	-39.257	-25.519	44.200
299.910	7089.782	-179.343	32.969	-52.124
-39.257	-179.343	1833.322	343.079	-594.230
-25.519	32.969	343.079	747.916	-270.769
44.200	-52.124	-594.230	-270.769	9276.223

no.	Energy	Mult.(total)	Mult.(Spin)	Mult.(Bahn)
1	.000	5	5	1
2	431.088	5	5	1
3	1655.452	5	5	1
4	6892.644	5	5	1
5	9118.458	5	5	1
6	17166.822	3	3	1
7	17580.372	3	3	1
8	18965.957	3	3	1
9	19397.533	3	3	1
10	20209.499	3	3	1
11	20250.241	3	3	1
12	20778.353	3	3	1
13	21235.648	3	3	1
14	21316.116	3	3	1
15	22051.937	3	3	1
16	22221.843	3	3	1
17	22591.456	3	3	1
18	22661.917	3	3	1
19	23923.432	3	3	1
20	23941.724	3	3	1
21	24450.551	3	3	1
22	24644.504	3	3	1
23	24761.703	3	3	1
24	24962.617	3	3	1

	energy(NEVPT2)	energy(calc.)	difference	weight
31	15593.000	17166.822	1573.822	1.000
31	16340.000	17580.372	1240.372	1.000
31	18806.000	18965.957	159.957	1.000
31	18977.000	19397.533	420.533	1.000
31	20631.000	20209.499	-421.501	1.000
31	20631.000	20250.241	-380.759	1.000
31	21282.000	20778.353	-503.647	1.000
31	21538.000	21235.648	-302.352	1.000
31	22096.000	21316.116	-779.884	1.000
31	22632.000	22051.937	-580.063	1.000
31	22768.000	22221.843	-546.157	1.000

Sigma, weighted = 746.420

NEXT CALCULATION WITH OPTIMIZED PARAMETERS

zeta = 821.954276
*
esig = 5291.000000
epis = 3414.000000
epic = 884.000000
B = 602.000000
C = 4364.000000

```
1        .000            1
  2      .072            1
  3     325.774            1
  4     330.940            1
  5     537.469            1
  6     925.496            1
  7    1067.246            1
  8    1252.741            1
  9    1523.451            1
 10    1524.610            1

energy (exp.)   energy(calc.)  difference    weight

1                78.100         325.774     247.674     1.000
1                84.900         330.940     246.040     1.000
1               111.200         537.469     426.269     1.000
1              1347.500         925.496    -422.004     1.000
1              1373.200        1067.246    -305.954     1.000
1              1384.400        1252.741    -131.659     1.000
1              1464.700        1523.451      58.751     1.000
1              1464.800        1524.610      59.810     1.000

Sigma, weighted =      273.779
```

Complex 7 Fe[N(CCH3)]2

```
NEXT CALCULATION WITH OPTIMIZED PARAMETERS

B          =   1833.533996
C          =   3030.579870
*
esig       =   3977.000000
epis       =   4530.000000
epic       =   2321.000000

AOM matrix

        xy        xz        yz      x2y2        z2

      .365    34.276    18.561      .093     -.297
    34.276  6774.630   402.192    26.327   -10.362
    18.561   402.192  6926.796   -14.393    14.879
      .093    26.327   -14.393      .275     -.148
     -.297   -10.362    14.879     -.148  7953.935


             energy(NEVPT2)   energy(calc.)  difference    weight

31             20176.000       20443.505     267.505     1.000
31             20309.000       20724.530     415.530     1.000
31             21542.000       21214.879    -327.121     1.000
31             21597.000       21508.945     -88.055     1.000
31             21688.000       21541.698    -146.302     1.000
31             21771.000       21652.027    -118.973     1.000
31             21858.000       21672.623    -185.377     1.000
31             22204.000       22541.143     337.143     1.000
31             22270.000       22543.898     273.898     1.000
31             22323.000       22565.895     242.895     1.000
31             23376.000       22679.234    -696.766     1.000

Sigma, weighted =      325.028
```

```
NEXT CALCULATION WITH OPTIMIZED PARAMETERS

zeta       =    591.085659
*
esig       =   3977.000000
epis       =   4530.000000
epic       =   2321.000000
B          =   1834.000000
C          =   3030.000000


           energy(NEVPT2)   energy(calc.)  difference    weight

1               122.800         294.768     171.968     1.000
1               172.200         585.461     413.261     1.000
1               937.600         585.473    -352.127     1.000
1               985.700         871.189    -114.511     1.000
1               986.800         873.318    -113.482     1.000
1              1106.700        1154.798      48.098     1.000
1              1106.800        1155.799      48.999     1.000

Sigma, weighted =      225.216
```

SI.15. Optimized geometries of FeX_2 model complexes (Fig.1) and $FeCl_2^{1+}$

NAME = fech32_pbe_opt_qro.inp
| 1> ! PBE VDW10 TZVP TZVP/J
| 2> !noautostart noiter moread normalprint
| 3> %moinp "fech32_pbe_opt.qro"
| 4>
| 5> *xyzfile 0 5 fech32_pbe_opt.xyz

CARTESIAN COORDINATES (ANGSTROEM)

Fe	-0.000000	0.000000	0.000000
C	-0.000183	0.000000	2.025151
C	0.000183	0.000000	-2.025151
H	-1.024491	-0.000002	2.437754
H	1.024491	-0.000002	-2.437754
H	0.512820	-0.886256	2.440171
H	0.512817	0.886258	2.440171
H	-0.512820	-0.886256	-2.440171
H	-0.512817	0.886258	-2.440171

INTERNAL COORDINATES (ANGSTROEM)

Fe	0	0	0	0.000000	0.000	0.000
C	1	0	0	2.025151	0.000	0.000
C	1	2	0	2.025151	180.000	0.000
H	2	1	3	1.104286	111.945	0.000
H	3	1	2	1.104286	111.945	0.000
H	2	1	3	1.104927	112.059	0.000
H	2	1	3	1.104927	112.059	0.000
H	3	1	2	1.104927	112.059	0.000
H	3	1	2	1.104927	112.059	0.000

```
NAME = fenh22_pbe_opt_qro.inp
|  1> # Model complex Fe(NH2)2
|  2> #
|  3> !PBE  TZVP TZV/J
|  4> !noautostart noiter moread normalprint
|  5> %moinp "fenh22_pbe_opt.qro"
|  6>
|  7>
|  8> *xyzfile  0  5  fenh22_pbe_opt.xyz
|  9>
| 10>
| 11>                         ****END OF INPUT****

CARTESIAN COORDINATES (ANGSTROEM)
---------------------------------
  Fe    -0.000000    0.000030    0.000000
  N     -0.000000    0.000029    1.856424
  N     -0.000000    0.000031   -1.856424
  H      0.828499   -0.000265    2.448922
  H     -0.828499    0.000220    2.448922
  H      0.828499    0.000220   -2.448922
  H     -0.828499   -0.000265   -2.448922

---------------------------------
INTERNAL COORDINATES (ANGSTROEM)
---------------------------------
 Fe    0   0   0   0.000000     0.000     0.000
 N     1   0   0   1.856424     0.000     0.000
 N     1   2   0   1.856424   180.000     0.000
 H     2   1   3   1.018560   125.570     0.000
 H     2   1   3   1.018560   125.570     0.000
 H     3   1   2   1.018560   125.570     0.000
 H     3   1   2   1.018560   125.570     0.000


                             INPUT FILE
================================================================================
NAME = feoh2_pbe_opt_qro.inp
|  1> # Model complex Fe(OH)2
|  2> #
|  3> ! TZVP TZV/J
|  4> !noautostart noiter moread normalprint
|  5> %moinp "feoh2_pbe_opt.qro"
|  6>
|  7>
|  8>
|  9>
| 10> *xyzfile  0  5  feoh2_pbe_opt.xyz
| 11>
| 12>
| 13>
| 14>
| 15>                         ****END OF INPUT****
```

CARTESIAN COORDINATES (ANGSTROEM)

Fe	-0.000000	0.000356	0.000000
O	0.047556	0.000357	1.792348
O	-0.047556	0.000357	-1.792348
H	0.832091	-0.000535	2.359706
H	-0.832091	-0.000535	-2.359706

INTERNAL COORDINATES (ANGSTROEM)

Fe	0	0	0	0.000000	0.000	0.000
O	1	0	0	1.792979	0.000	0.000
O	1	2	0	1.792979	180.000	0.000
H	2	1	3	0.968190	127.393	269.934
H	3	1	2	0.968190	127.393	269.934

==
INPUT FILE
==
NAME = fe3cl2_bent_opt_qro.inp
| 1> ! PBE TZVP TZV/J
| 2> !noautostart noiter moread normalprint
| 3> %moinp "fe3cl2_bent_opt.qro"
| 4>
| 5> *xyzfile 1 6 fe3cl2_bent_opt.xyz
| 6>
| 7>
| 8>
| 9>
| 10> ****END OF INPUT****
==

CARTESIAN COORDINATES (ANGSTROEM)

Fe	0.000000	0.000000	-0.425386
Cl	1.910929	0.000000	-1.271307
Cl	-1.910930	0.000000	-1.271307

INTERNAL COORDINATES (ANGSTROEM)

Fe	0	0	0	0.000000	0.000	0.000
Cl	1	0	0	2.089792	0.000	0.000
Cl	1	2	0	2.089793	132.244	0.000